Direct Dynamics Studies of CO-Assisted Carbon Nanotube Growth

David J. Mann* and Mathew D. Halls

Scientific Simulation and Modeling Group, Zyvex Corporation, Richardson, Texas 75081

William L. Hase

Department of Chemistry and Institute for Scientific Computing, Wayne State University, Detroit, Michigan 48202

Received: January 30, 2002; In Final Form: August 6, 2002

Semiempirical direct dynamics simulations are used to study the potential role of CO in the gas-phase catalytic growth of carbon nanotubes. Calculations employing a fully self-consistent AM1 semiempirical electronic Hamiltonian predict that CO molecules can chemically adsorb to the open edge of partially grown zigzag and armchair nanotubes. The adsorbed CO molecules can form either pentagonal or hexagonal carbon rings by an electrocyclic reaction with neighboring adsorbed CO groups. Formation of hexagonal carbon rings in zigzag nanotubes is kinetically and thermodynamically favored by a CO insertion reaction with CO-saturated ends. These results provide some computational evidence that gas-phase CO can adsorb and contribute to the intermediate and latter stages of carbon nanotube growth. This study assumes that growth proceeds by the addition of carbon to the nanotube edge held open by metal catalyst particles, as opposed to a root growth or capped end growth mechanism.

1. Introduction

Carbon nanotubes,[1] in particular single-walled nanotubes (SWNTs), are a material that has been rigorously studied both experimentally[2−8] and theoretically[9−12] during the past few years. Their popularity is due, in large part, to the wide range of possible applications made by exploiting their unique structural, electronic, and mechanical properties.[13,14] Their use as scanning tunneling microscope tips,[15] quantum wires,[16] and electronic rectifying nanodevices[17] has already been reported in the literature. Future applications involve use as carbon matrix composites[18] and chemical reaction vessels.[19] For the latter, the effects of confinement and polarizability may be a means of enhancing and controlling chemical reactivity occurring inside a SWNT.[20] These effects are expected to be heavily dependent upon the structure and type of nanotube, such as tube diameter and chirality; thus, methods for synthesizing specific types of nanotubes are needed.

During the past few years, much progresss has been made in the synthesis of carbon nanotubes, in particular newly developed procedures for producing batches consisting entirely of SWNTs. The gas-phase catalytic growth of SWNTs from carbon monoxide (CO) is a procedure developed by Smalley that has shown great promise as a means of controlling the yield and diameter distribution of SWNTs.[21−25] In the HiPco (high-pressure CO disproportionation) process, $Fe(CO)_5$ is injected into a stream of CO gas at high temperature and pressure.[22,23] The iron forms metal clusters that act as catalytic sites to promote the Boudouard reaction:

$$CO + CO \rightarrow C(s) + CO_2(g)$$

It is believed that the slow bimolecular Boudouard reaction limits the carbon supply to the growing carbon structure so that only the most energetically favorable carbon structures form, such as SWNTs.[22,24] When the carbon-covered metal clusters reach a size near that of C_{60}, they nucleate and grow SWNTs.[23] The growth is terminated when the metal cluster reaches a size that favors formation of a carbon shell around the cluster[23] or when curvature-inducing defects are formed, such as adjacent pentagon pairs.[26]

Although it may be possible for a single mechanism to control the growth of SWNTs in the HiPco process, it is worth investigating the possibility that different mechanisms come into play at different stages of tube growth. Once growth is initiated from the assembly of carbon atoms generated via CO disproportonation, a more fundamental question is whether extended growth requires catalytically reduced carbon atoms as the carbon supply. One possibility that we propose here is that once growth is initiated gas-phase CO molecules might be able to assemble at the open edge of partially grown SWNTs and contribute to tube growth without having to first become reduced to C and CO_2. Vander Wal et al.[27] found that increasing the concentration of the CO feedstock gas has no apparent effect on nanotube yield but does lead to longer nanotubes. If the role of the catalyst becomes less important after growth has been initiated and if CO assembly with the nanotube ends can contribute to extended growth, the nanotubes would be expected to grow to longer lengths with an increased CO/Fe ratio.

To investigate the likelihood of CO-assisted carbon nanotube growth, we have carried out a detailed study using semiempirical direct dynamics simulations. The semiempirical Hartree−Fock (HF) molecular orbital (MO) theories based upon the neglect of diatomic differential overlap (NDDO) method have been used successfully over the years in many theoretical studies.[28−31] The most accurate of the NDDO methods are the AM1[32] and PM3[33] parametrized Hamiltonian models of Dewar and Stewart, respectively. In a recent theoretical dynamics study of the oxidation of carbon nanotubes,[34] the AM1 model was found to

10.1021/jp0255435 CCC: $22.00
Published on Web 11/12/2002

be qualitatively accurate compared to higher level first-principles methods. Because of the similarity of these two systems, the AM1 method was chosen for this study.

To explore CO-assisted tube growth, simulations involving three separate growth stages are examined: the adsorption of CO to the edge of a partially grown nanotube, formation of hexagonal carbon rings, and reduction of a resulting oxygen-containing nanotube. Semiempirical direct dynamics simulations provide a means of exploring each of these growth stages for models consisting of up to 100 atoms for tens of picoseconds (ps). It has already been shown from both experimental and theoretical studies that nanotube growth is facilitated by the presence of metal catalyst.[35,36] The metal particles have the effect of stabilizing the open-end nanotube allowing for additional assembly of carbon atoms without undergoing spontaneous tube closure. The tube closure mechanism was first identified from Car−Parinello studies of a (10,0) SWNT in the absence of catalyst particles at elevated temperatures, supporting an open-end growth mechanism of SWNTs.[37] Alternatively, a root growth mechanism has recently been reported.[52] In related work by Hernandez et al.,[38] the effects of boron on the assistance of tube growth were examined using semiempirical tight-binding molecular dynamics simulations. They found that boron stabilizes the edge of zigzag nanotubes delaying the tube closure process. This result provided some explanation for the experimentally observed improved aspect ratio in nanotubes synthesized in the presence of boron. Given the different procedures for nanotube production and different predictions regarding the precise growth mechanism, there may not exist a single common mechanism for nanotube growth. Moreover, the role of the catalyst may differ depending on the synthesis procedure. In our study, we have neglected the presence of the iron catalyst and instead focus on the assembly process through studies of the chemical reactions between CO and partially grown open-end nanotubes.

2. Computational Details

Classical trajectories are computed directly on the AM1 semiempirical HF potential energy surface (PES). A constant-temperature molecular dynamics (MD) and quasi-classical trajectory code was developed and incorporated into the GAMESS electronic structure program,[39] in which some of the algorithms were extracted from the general chemical dynamics program VENUS.[40] All simulations performed in this study were carried out under conditions of constant temperature using a 10 thermostat Nosé−Hoover chain algorithm.[41] The VV1 velocity verlet algorithm of Jang and Voth[42] was used for numerically integrating the Nosé−Hoover chain equations with an integration time step of 0.5 fs.

The simulation models used in this study consist of the (4,4) armchair and (6,0) zigzag nanotubes, as shown in Figure 1, left and right panels, respectively. One end of the nanotube is terminated with H atoms, while the other end is left open representing a partially grown nanotube. In all of the simulations reported in this study, the terminal H atoms are constrained to their equilibrium positions over the duration of the simulation. The equilibrium geometries of the starting structures were obtained by performing structural relaxations using the efficient quasi-Newton optimizer of Schlegel.[43]

Because these simulations are carried out within the *NVT* ensemble, the initial coordinates and velocities should be chosen from a thermal Boltzmann distribution to avoid equilibration. This was accomplished by using the accurate quasi-classical normal mode sampling procedure[44,45,46] in which the normal mode quantum numbers are sampled from a thermal Boltzmann distribution at the simulation temperature, *T*. A random phase is assigned to each normal mode, and the resulting normal mode coordinates and velocities are transformed into their Cartesian counterparts through a linear transformation using the normal mode eigenvectors. Because the H atoms are constrained throughout the simulation, they are held fixed to their equilibrium positions during the normal mode transformation and assigned an initial velocity of zero. A spurious angular momentum arises from this transformation and is subtracted from the system so that there is no net rotational energy. A more thorough description of the quasi-classical sampling procedure has been given elsewhere.[47,48]

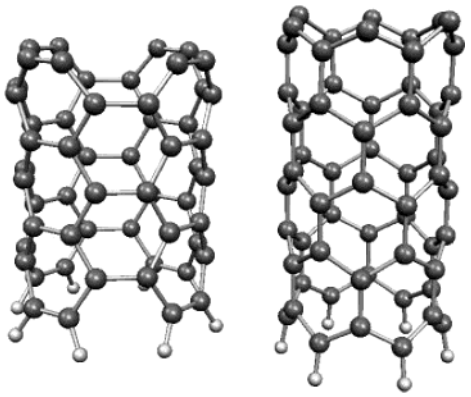

Figure 1. Model of the (4,4) armchair (left) and (6,0) zigzag (right) nanotubes terminated with H atoms at one end.

The simulation temperature of 2000 K employed here is more than 500 K higher than the largest temperature of 1200 °C (1473 K) used in the growth experiments of Smalley and co-workers.[22] This is done in an attempt to reduce the CPU time for observing chemistry by enhancing the overall reactivity. In their experiments, they found that the largest yields were obtained at the highest accessible temperature (1200 °C); therefore, our simulation temperature is realistic within this context.

3. Results and Discussion

3.1. Adsorption of CO to the Nanotube Edge. During the gas-phase catalytic growth process, any excess CO that does not decompose into C and CO_2 has potential for reaction with the partially grown nanotube. An encounter of CO with the nanotube edge could lead to the formation of a C−C bond between the nanotube and CO carbons, a C−O bond between the nanotube carbon and CO oxygen, or both. To investigate these possible modes of adsorption, we first calculate the adsorption energies for the configurations illustrated in Figure 2. These adsorption configurations correspond to an adatom and a 1,4-adsorption to the (4,4) nanotube and an adatom and a 1,3-adsorption to the (6,0) nanotube, as depicted in Figure 2, parts a, b, c, and d, respectively. A full unconstrained geometry optimization of each of these configurations is performed, and the adsorption energy relative to the energy of the nanotube plus CO at infinite separation is calculated according to the expression

$$E_{ads} = E_{tube+CO} - (E_{tube} + E_{CO}) \quad (1)$$

For the case of CO adsorption to the (6,0) nanotube edge, the adsorption energy of −90.0 kcal/mol for horizontal 1,3-addition is almost 6 kcal/mol more exothermic than that for adatom adsorption (−84.4 kcal/mol). For the case of CO adsorption to the (4,4) nanotube edge, the adatom adsorption energy of −55.9

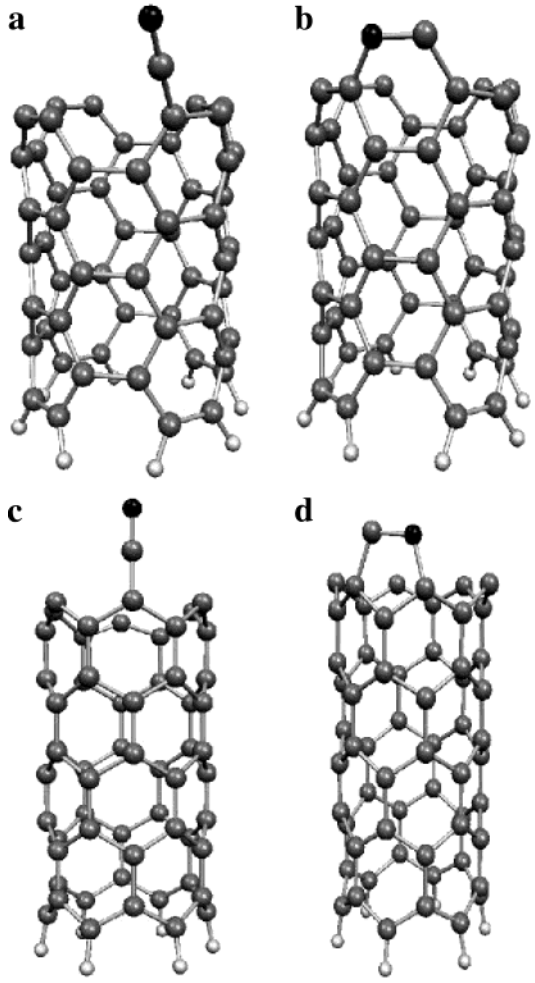

Figure 2. Structures obtained after adsorption of one CO molecule to the edge of the (4,4) and (6,0) nanotubes: (a) adatom adsorbed CO to (4,4) nanotube; (b) 1,4-addition of CO to (4,4) nanotube; (c) adatom adsorbed CO to (6,0) nanotube; (d) 1,3-addition of CO to (6,0) nanotube. Shown are the carbon atoms in gray and the oxygen atom in black.

kcal/mol is substantially larger than the 1,4-adsorption energy of −22.7 kcal/mol. The structure of the adatom adsorption products contains a C═C═O ketene-like[49] cumulated functional group terminating the nanotube end, whereas the product of 1,4-addition to the (4,4) nanotube has the CO σ-bonded to the terminal carbon atoms representing a six-membered ring containing one oxygen heteroatom. For the case of 1,3-addition to the (6,0) nanotube, both the CO carbon and the CO oxygen are double-bonded to the terminal carbon atoms of the nanotube, forming a five-membered ring with one oxygen heteroatom. This is the likely origin of the small 5.6 kcal/mol stronger binding energy for 1,3-adsorption to the (6,0) nanotube edge, compared to adatom adsorption. For adsorption to the (4,4) armchair nanotube edge, the formation of a C═C double bond by adsorbed CO in the adatom product is a likely origin of the 30.9 kcal/mol energy difference between these two adsorption configurations. The thermodynamic efficiency of subsequent adsorption was investigated by calculating the binding energies for two and three CO molecules bonded to the terminal carbon atoms. The results are summarized in Table 1. We find that the adsorption of additional CO molecules to the nanotube edge is highly thermodynamically favorable.

Given the high exothermicity of CO adsorption to the (6,0) nanotube edge and adatom adsorption to the (4,4) nanotube edge, it seems likely that CO binds to the nanotube edge with either a small barrier or without a barrier. We estimated the adsorption barrier for the adatom addition of a single CO molecule to the (4,4) nanotube edge by performing a series of constrained optimizations. This was achieved by constraining the distance between the CO carbon and the nanotube carbon and incrementing this distance in inervals of 0.1 Å, starting from the adsorption minima. A similar set of calculations were performed for 1,3-addition to the (6,0) nanotube edge by constraining the distance between the CO bond axis and the axis connecting the two terminal nanotube carbon atoms. A plot of the energies along these approximate reaction coordinates, measured relative to their corresponding adsorption minima, is shown in Figure 3. The energy smoothly increases to the value at infinite separation between the nanotube and CO with no evidence of an adsorption barrier. This result is consistent with the findings of Lee and co-workers[50] for adsorption of O_2 to the nanotube edge (i.e., barrierless adsorption) using density functional theory. On the basis of these results, we predict that an encounter of CO with the nanotube during intermediate growth stages will lead to the spontaneous adsorption of CO with the nanotube edge, culminating in structures analogous to those depicted in Figure 2. The fate of adsorbed CO to the nanotube edge will be discussed in the remaining sections of this paper.

TABLE 1: RHF/AM1 CO Adsorption Energies to the (6,0) and (4,4) Nanotube Edges

nanotube	adsorption type	no. of CO's	E_{ads} (kcal/mol)
(6,0)	adatom	1	−84.4
(6,0)	1,3-addition	1	−90.0
(6,0)	1,3-addition	2	−162.2
(6,0)	1,3-addition	3	−226.9
(4,4)	adatom	1	−55.9
(4,4)	1,4-addition	1	−22.7
(4,4)	adatom	2	−99.6
(4,4)	adatom	3	−171.3

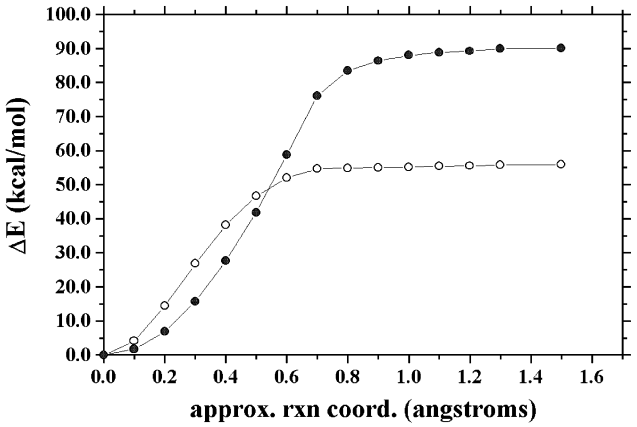

Figure 3. Plots of the energies versus an approximate reaction coordinate for the (○) adatom adsorption of CO to the edge of the (4,4) nanotube and (●) 1,3-addition to the edge of the (6,0) nanotube.

3.2. Dynamics of Adsorbed CO. The possibility of CO-assisted tube growth will be largely dependent upon the motion of the CO molecule following adsorption to the nanotube edge. Interconversion between the adatom and heterocyclic configurations, CO migration along the nanotube edge, and diffusion along the nanotube sidewalls are three possible dynamical events that could either aid, inhibit, or not affect gas-phase catalytic tube growth. Four separate simulations were carried out at a temperature of 2000 K for 10 ps using the methods described in section 2 starting from the following configurations: adatom addition to the (4,4) nanotube, 1,4-addition to the (4,4) nanotube, adatom addition to the (6,0) nanotube, and 1,3-addition to the

(6,0) nanotube. In each trajectory, the motion of the CO molecule is probed over the duration of the simulation.

We start with an explanation of the dynamics of CO adsorbed to the (4,4) armchair nanotube. In the first simulation, we started from the 1,4-addition product (Figure 2b) and activated the vibrational modes with quasi-classical normal mode sampling. The CO molecule bound to the nanotube in this configuration is unstable and quickly converts to the adatom addition product (Figure 2a) after 540 fs of dynamics. Rather than propagate this trajectory for the full 10 ps, we halted it, and four additional short time trajectories were calculated to explore the effects of initial conditions on the rapid interconversion to the adatom addition product. From the four additional trajectories, we found that interconversion to the adatom addition product occurs after 370, 480, 620, and 830 fs, suggesting a small barrier to conversion from the 1,4-addition to adatom adsorption product. Each trajectory was integrated for 2 ps without observation of barrier recrossing; the CO remains in the adatom addition configuration. One interesting result is that in three of these simulations the CO "hops" to the adjacent terminal carbon of the nanotube following conversion to the ketene product. We investigated the mobility of CO along the nanotube edge more extensively with a single long-time simulation starting from the adatom adsorption configuration. Similarly, we observed multiple site exchange between the two terminal carbon atoms of the nanotube along the terminal C−C bond axis. This exchange occurs by passing through a three-membered carbon ring transition state, apparently with a relatively small barrier. We did not, however, observe CO migration to a nearby terminal C−C bond (i.e., to an adjacent terminal carbon hexagon). Snapshots from this simulation, illustrating the CO site exchange mechanism, are shown in Figure 4 in which the short-lived three-membered-ring transition structure appears in the second snapshot.

We found very different behavior for the dynamics of CO chemisorbed to the edge of the (6,0) nanotube. Starting from the most stable adsorption configuration (the horizontal 1,3-addition product shown in Figure 2d), we carried out a 10 ps simulation at 2000 K with quasi-classical normal mode sampling. After 3.4 ps, the C−O bond (originally part of CO) dissociates without associating to regenerate the 1,3-adsorbed configuration. Dissociation of CO at the nanotube edge is a very important result and could be a key step in the potential CO-assisted growth mechanism. We expect that under experimental conditions of high CO temperature and pressure that a collision of CO with the nanotube edge could enhance dissociation via collision to vibrational energy transfer. We did not, however, carry out any of these simulations for this initial study; instead, the primary focus is on the chemistry and dynamics of adsorbed CO.

In the second long-time simulation, we started from the adatom adsorption configuration (as depicted in Figure 2c). Here, we were primarily interested in whether the vertically adsorbed CO molecule interconverts to the horizontal 1,3-adsorption configuration via electrocyclization or undergoes similar site exhange as for the case of adsorbed CO to the armchair nanotube. What we found is that neither of these two reactions occur. Rather, after 1.3 ps, the chemisorbed CO cyclizes with a neighboring terminal carbon to form a four-membered cyclobutanone terminal ring. The structure remains up to 5.1 ps and then reopens as the CO completely exchanges to the neighboring terminal carbon. The dynamics of adatom-adsorbed CO to the zigzag nanotube appears very similar to the armchair case, suggesting a relatively high mobility of CO along the nanotube edge.

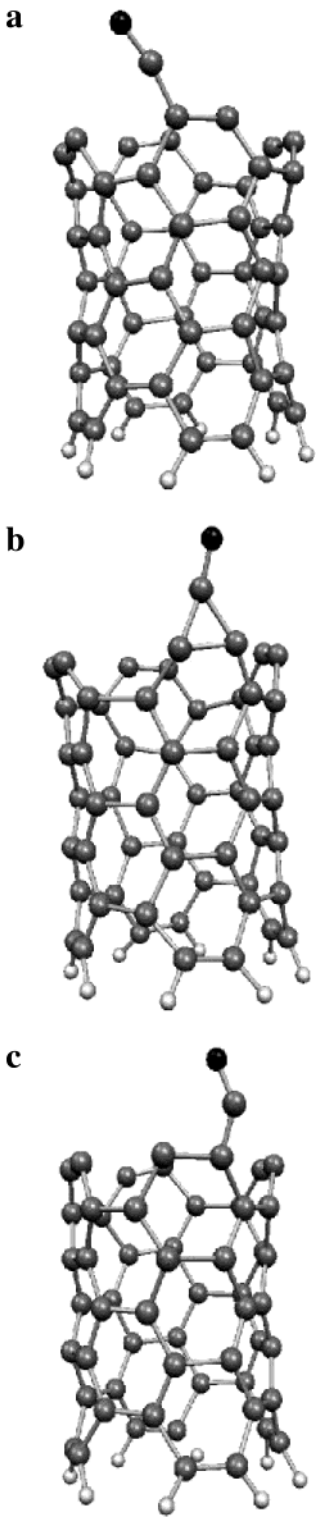

Figure 4. Snapshots illustrating the dynamics of adatom adsorbed CO to the edge of the (4,4) armchair nanotube for a 10 ps simulation at 2000 K: (a) initial structure; (b) cyclic intermediate separating CO site exchange; (c) CO exchanging sites along the nanotube edge. Shown are the carbon atoms in gray and the oxygen atom in black.

3.3. Carbon Ring Formation from Adsorbed CO. The growth of carbon nanotubes via adsorbed CO will require the formation of either five- or six-membered carbon rings. Under actual experimental conditions, during which highly reactive carbon atoms are present from reduction of CO, a whole series of complex reactions occurring through the cooperative involvement of CO and C atoms can take place. This type of cooperative assembly may contribute to the mechanism of CO-

assisted nanotube growth, but because of the complexity of modeling the large array of potential reactions, we have only considered ring formation through neighboring adsorbed CO molecules in this study.

To properly model ring formation, we have only considered fully saturated nanotube edges. Because of the relatively high mobility of adatom-adsorbed CO along the nanotube edge, this eliminates CO migration to nearby sites, which would delay possible chemistry between neighboring CO molecules. The four systems that we have considered in this study are the following: (i) a fully saturated (6,0) nanotube consisting of a total of six adatom-adsorbed CO molecules to the edge, (ii) a fully saturated (6,0) nanotube consisting of three CO molecules 1,3-adsorbed to the edge, (iii) the same as ii but with an additional gas-phase CO inserted at the edge, and (iv) a fully saturated (4,4) nanotube consisting of eight adatom-adsorbed CO molecules to the edge. For each of these four systems, we started by calculating a single trajectory at a temperature of 2000 K, using the methods described in section 2, for a total time of 10 ps.

In our first simulation, we modeled the (6,0) nanotube containing six CO molecules adatom-adsorbed to the nanotube edge. The intial conditions were determined by quasi-classical normal mode sampling at a temperature of 2000 K, and the trajectory was propagated for 10 ps at this temperature. The initial structure of this system is shown in Figure 5a. After approximately 1.1 ps, two neighboring adsorbed CO molecules cyclize to form a six-membered oxygen-containing heterocyclic ring, resembling a cycloester. The snapshot from this trajectory after 1.1 ps is shown in Figure 5b. After 2.7 ps of dynamics, two neighboring CO molecules on the opposite side of the heterocyclic ring cyclize generating a five-membered carbon ring terminated with two oxygen atoms. This snaphsot is shown in Figure 5c. Interestingly, both cyclic rings remain after 10 ps of dynamics, and furthermore, the observation of carbon ring formation via adsorbed CO is found to be possible. The ultimate fate of the oxygen heterocycle is not known until further simulations are carried out. However, we can speculate as to what might happen if subsequent CO molecules react with the heterocyclic ring. One possibility is the addition of CO to a neighboring C atom site, later inserting itself inside the ring replacing the O atom and generating a six-membered carbon ring. A second case could involve the direct addition of CO to the O heteroatom, later re-opening the ring and eliminating CO_2. This has the effect of reducing of the oxygenated nanotube leaving a highly reactive bare terminal carbon atom.

Because 1,3-addition to the zigzag nanotube edge is the thermodynamically most favorable reaction pathway, we chose to carry out an additional simulation considering a case in which the nanotube is saturated with CO adsorbed in this way. The simulation was carried out in the exact same manner as above with the initial structure shown in Figure 6a. The results from this 10 ps trajectory are found to be very different from that observed in the adatom adsorption case. After 1.4 ps, dissociation of the CO bond (reminiscent of the single CO molecule studies) occurs. A snapshot at 1.4 ps is shown in Figure 6b. After 2.1 ps, a different type of cyclization occurs in which two carbon atoms from neighboring adsorbed CO molecules join to form a five-membered carbon ring. The dissociated CO bond and the pentagonal carbon ring remain after 10 ps (snapshot shown in Figure 6c). As with the previous simulation, we find that the formation of carbon rings via adsorbed CO is possible out of two different configurations considered. To extend this study further, additional simulations consisting of randomly adsorbed CO to the nanotube edge could shed some additional light on potential ring-forming reactions that might occur. Currently, such studies are in progress.

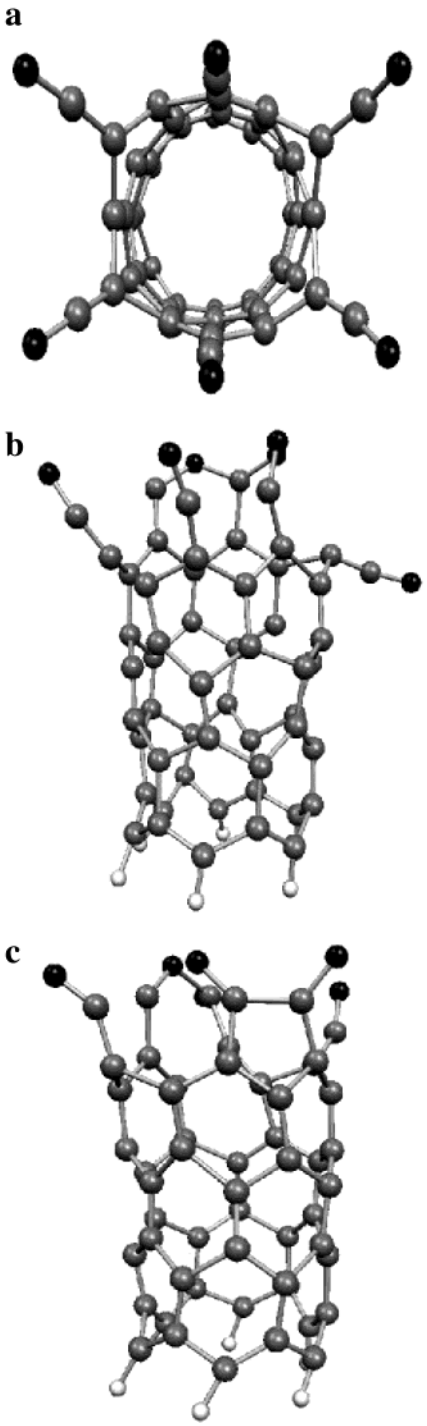

Figure 5. Snapshots of a 10 ps simulation of six adatom adsorbed CO molecules to the edge of the (6,0) nanotube: (a) initial structure of the saturated nanotube (top view); (b) snapshot after 1.1 ps depicting formation of a six-membered oxygen-containing heterocyclic ring; (c) snapshot after 2.7 ps when formation of a five-membered pentagonal carbon ring occurs. Shown are the carbon atoms in gray and the oxygen atoms in black.

On the basis of these limited numbers of simulations, electrocyclic ring formation of adsorbed CO at the edge of a zigzag nanotube is only discovered to yield five-membered carbon rings. Alternatively, six-membered rings could conceivably form atop zigzag nanotubes by inserting a fourth CO at the saturated edge of the system shown in Figure 6a. To model

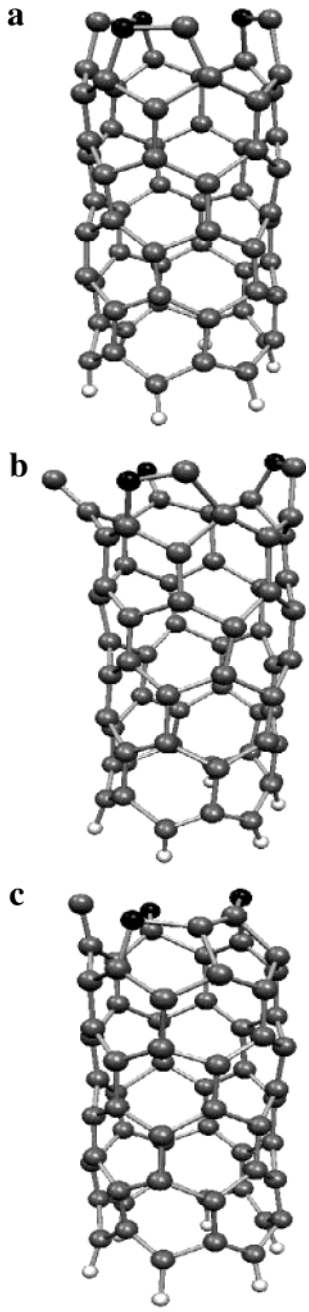

Figure 6. Snapshots of a simulation consisting of three CO molecules adsorbed to the edge of the (6,0) nanotube via 1,3-addition: (a) initial structure; (b) snapshot after 1.4 ps illustrating dissociation of a CO bond of an adsorbed CO molecule; (c) snapshot after 2.1 ps depicting pentagonal carbon ring formation via electrocyclization. Shown are the carbon atoms in gray and the oxygen atoms in black.

this reaction, we placed a CO molecule 5 Å above the saturated nanotube edge (with the CO carbon oriented toward the nanotube) and assigned a small incident energy of 4 kcal/mol (the Boltzmann average translational energy at 2000 K) projected toward the center of two adsorbed CO molecules. Snaphots from this simulation are shown in Figure 7. The CO molecule is found to quickly insert itself between the two adsorbed CO carbon atoms forming a new hexagonal carbon ring. This newly formed ring structure was found to be stable over the duration of the 5.0 ps simulation, and total energy calculations revealed that this insertion reaction is highly exothermic with a reaction energy of −107.9 kcal/mol. A series of constrained optimizations, similar to those performed in section III, predict this reaction to occur without an energy

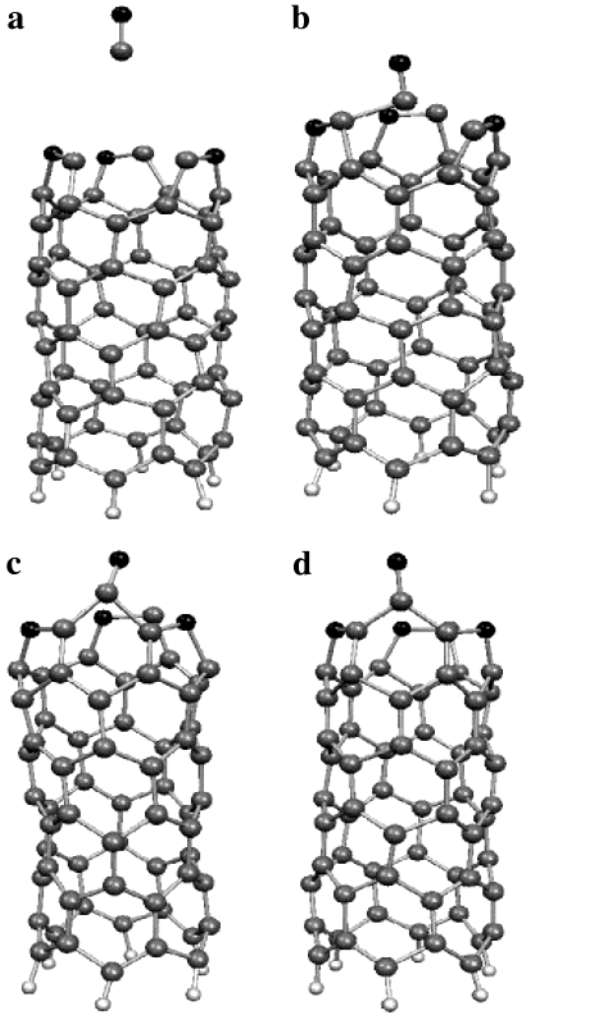

Figure 7. Simulation at 2000 K of the adsorption of a fourth CO molecule to the edge of the CO saturated nanotube system depicted in Figure 6: (a) snapshot of the system after 30 fs initiated with a CO incident energy of 4 kcal/mol; (b) insertion of CO between two CO carbon atoms forming a new C−C bond; (c) formation of second C−C bond generating new hexagonal carbon ring; (d) snapshot after 10 ps of dynamics. Shown are the carbon atoms in gray and the oxygen atoms in black.

barrier. Hence, a sequence of adsorption reactions leading to this new six-membered carbon ring all occur without a barrier.

We have investigated the effect of CO orientation on the insertion step by performing a series of simulations with a random orientation assigned to CO given a thermal incident energy of 4 kcal/mol. The objective of these simulations is to identify all possible reaction pathways (under thermal conditions) for the encounter of CO to the edge of a CO adsorbed saturated nanotube and whether any additional precursor steps significantly slow the rate of insertion, allowing for competition with electrocyclization. For cases in which the CO oxygen first encounters the nanotube edge (either with a terminal C or O atom), no reaction is observed and the CO molecule reorients itself, leading to the same structure shown in Figure 7a. However, for the case in which the CO carbon associates with a terminal O atom, a CO_2 substituent forms; this may be an important step for the removal of O atoms from the saturated nanotube edge allowing for the assembly of additional CO molecules.

The detailed picture of CO assembly and nanotube growth is expected to proceed through random self-assembly of CO molecules at the nanotube edge followed by either insertion

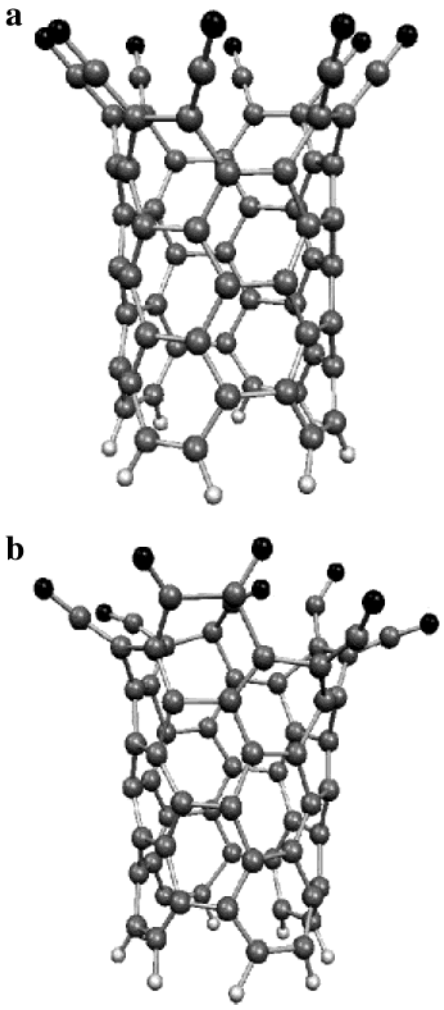

Figure 8. Minimum energy structure of (a) eight CO molecules bound adatom to the edge of the (4,4) nanotube and (b) snapshot after 6.9 ps of a 10 ps simulation of this system at 3000 K. Shown are the carbon atoms in gray and the oxygen atoms in black.

between two adjacent adsorbed CO molecules, leading to a new hexagonal carbon ring, or association with an adsorbed CO terminal oxygen atom, whereby a CO_2 substituent forms and, possibly, detaches from the nanotube producing CO_2. A complete growth mechanism could be determined through a detailed kinetic analysis of all possible reactions coupled with kinetic Monte Carlo simulations, which have already been used in modeling carbon nanotube growth.[51]

In our final simulation, we have modeled potential CO-assisted carbon ring formation with the (4,4) armchair nanotube. Starting from a nanotube fully saturated with CO and activating with quasi-classical normal mode sampling, we carried out a 10 ps simulation at 2000 K. We did not observe any reactions from this single trajectory. This is partially attributed to the greater space neighboring adsorbed CO groups have to extend to cyclize. In addition, we observed from the simulation that the CO groups have a tendency to populate the outer tube region rather than occupying the inner tube region where reactions might be more favorable, particularly electrocyclization. We then carried out a second simulation, this time at a much higher temperature of 3000 K. At this higher temperature, the encounter frequency between nearby adsorbed CO groups (as well as the cyclization attempt frequency) is found to be much more extensive. After 6.9 ps, one cyclization reaction occurs forming a hexagonal carbon ring (as shown from the second snapshot in Figure 8).

3.4. Extended Nanotube Growth. The growth model outlined above implies that CO molecules can adsorb to the open edge of SWNTs and contribute to nanotube growth by forming hexagonal carbon rings. Although our simulations have only concentrated on CO molecules chemically adsorbed to the open edge, the fact that carbon atoms (or C_2 dimers) are also expected to be present from CO disproportionation suggests a possible cooperative mechanism involving both carbon atoms and CO molecules. Kiang proposed a microscopic growth mechanism whereby growth occurs through the addition of C_2 dimers as opposed to single carbon atoms.[53] It is therefore conceivable that the oxygen-terminated nanotube can be reduced by reaction with C_2 dimers. Calculations with an additional carbon atom added to a terminal oxygen atom show that the resulting CO group can either desorb (due to the weak CO−C bond) or reorient leading to a new C−C bond (through an OC−C linkage). A similar situation is encountered if a C_2 dimer is added at the edge in place of the additional single carbon atom.

3.5. Presence of Catalyst Particles. Although our simulation models lack the presence of metal catalyst particles, the role of the metal particles is known to be critical for catalyzing the growth of SWNTs. If the adsorption of CO to the metal catalyst is thermodynamically favored over adsorption to the edge of an open-ended SWNT, the conclusions drawn thus far may be invalid. To address this question, we have calculated and compared the binding energies for CO adsorption to a small iron cluster (Fe_{16}) and the (6,0) zigzag nanotube. Because the semiempirical model used in this study cannot accurately represent metal clusters such as iron, the binding energies were determined from more accurate ab initio methods. Structural and energy minimizations were carried out within the generalized gradient approximation (GGA) of density functional theory using the functional of Perdew and Wang (PW91). The valence electrons were described using a plane-wave basis in conjunction with the ultrasoft Vanderbilt pseudopotentials of Kresse and Hafner,[56] as implemented in the Vasp code.[57] Integration over the Brillouin zone is performed using a single *k*-point. An energy cuttoff of 300 eV was used in all calculations for both the iron cluster and armchair nanotube.

The calculated binding energy of −28.5 kcal/mol for the adsorption of a single CO molecule to the Fe_{16} cluster is significantly smaller than the corresponding binding energy of −86.0 kcal/mol for adatom adsorption to the edge of the (6,0) SWNT. This finding suggests that adsorption of CO to the open edge of a SWNT is more favorable than adsorption to an Fe cluster and, therefore, concludes that the presence of Fe particles in the simulation model will not affect the simulation results. Furthermore, the semiempirical binding energy of −84.4 kcal/mol for CO adsorption to the (6,0) SWNT is in excellent agreement with the ab initio result of −86.0 kcal/mol, lending support to the accuracy of the semiempirical model for this system.

4. Conclusions

The primary assumption that we have made in this study is that growth proceeds through addition of carbon atoms to an open edge, as opposed to either addition to a capped end or root growth. The actual growth mechanism is a highly debated issue, and experimental evidence exists to support each. In a recent study, it was proposed that the root growth mechanism is common for all synthesis techniques,[52] which would include HiPco growth. Root growth occurs by the precipitation of carbon atoms from solvated metal clusters that assemble at the surface of the metal cluster growing carbon nanotubes. High-resolution

transmission electron microscopy images lend support to this type of mechanism.[52] However, similar images have yet to be shown for HiPco-grown SWNTs. Experimental evidence also exists that supports an open-end growth mechanism, whereby the catalyst serves to keep the nanotube opened at the end allowing for the capture of carbon atoms.[53−55] Although it would be desirable if there existed a single growth mechanism common to every gas-phase synthesis procedure, the possibility still remains that multiple growth mechanisms exist. Furthermore, it is possible that different mechanisms (or competing mechanisms) come into play at different stages of the growth.

The growth mechanism that we propose here is not an alternative to the already proposed mechanisms but merely represents a possible sequence of chemical reactions that could take place during the intermediate stages of HiPco growth. If HiPco growth proceeds through an open-edged nanotube then the highly reactive CO molecules are capable of adsorbing to the edge, leading to the formation of either pentagonal or hexagonal carbon rings, all without any energy barrier. Future studies aim at exploring, in more detail, the range of chemical reactions that can take place at the edge with more complex systems that contain encapsulated catalyst particles. If the formation of hexagonal rings is shown to be more energetically and kinetically favorable, then CO adsorption could contribute to extended growth. Otherwise, if pentagonal ring formation from CO adsorption is more favorable, then this proposed mechanism might help explain how growth termination takes place, because pentagons constitute a curvature-induced defect leading to tube closure. Some of the results reported in this paper may be experimentally verifiable by opening the ends of capped nanotubes and subjecting them to a CO feedstock gas. Observing extended growth in the absence of catalyst particles would verify the theoretical predictions made in this study.

Acknowledgment. The authors thank Wayne State University for providing computer support and H. B. Schlegel for helpful discussions with the manuscript. Michael J. Weller is also acknowledged for providing technical assistance. William L. Hase thanks the Office of Naval Research for financial support.

References and Notes

(1) Iijima, S. *Nature* **1991**, *354*, 56.
(2) Ouyang, M.; Huang, J.-L.; Cheung, C. L.; Lieber, C. M. *Science* **2001**, *292*, 702.
(3) Nagasawa, S.; Yudasaka, M.; Hirahara, K.; Ichihashi, T.; Iijima. S. *Chem. Phys. Lett.* **2000**, *328*, 374.
(4) Zhang, M.; Yudasaka, M.; Nihey, F.; Iijima, S. *Chem. Phys. Lett.* **2000**, *328*, 350.
(5) Tang, Z. K.; Zhang, L.; Wang, N.; Zhang, X. X.; Wen, G. H.; Li, G. D.; Wang, J. N.; Chan, C. T.; Sheng, P. *Science* **2001**, *292*, 2462.
(6) Rueckes, T.; Kim, K.; Joselevich, E.; Tseng, G. Y.; Cheung, C.-Li.; Lieber; C. M. *Science* **2000**, *288*, 94.
(7) Kim, P.; Lieber, C. M. *Science* **1999**, *286*, 2148.
(8) Zhou, C.; Kong, J.; Yenilmez, E.; Dai, H. *Science* **2000**, *290*, 1552.
(9) Farajian, A. A.; Ohno, K.; Esfarjani, K.; Maruyama, Y.; Kawazoe, Y. *J. Chem. Phys.* **1999**, *111*, 2164.
(10) Buldum, A.; Lu, J. P. *Phys. Rev. B* **2001**, *63*, 161403.
(11) Jhi, S.-H.; Louie, S. G.; Cohen, M. L. *Phys. Rev. Lett.* **2000**, *85*, 1710.
(12) Srivastava, D.; Brenner, D. W.; Schall, J. D.; Ausman, K. D.; Yu, M.; Ruoff, R. S. *J. Phys. Chem. B* **1999**, *103*, 4330.
(13) Saito, R.; Dresselhaus, G.; Dresselhaus, M. S. *Physical Properties of Carbon Nanotubes*; Imperial College Press: London, 1998.
(14) Endo, M.; Iijima, S.; Dresselhaus, M. S. *Carbon Nanotubes*; Elsevier Science Ltd.: Tarrytown, NY, 1996.
(15) Wong, S. S.; Harper, J. D.; Lansbury, P. T.; Lieber, C. M. *J. Am. Chem. Soc.* **1998**, *120*, 603.
(16) Tans, S. J.; Devoret, M. H.; Dai, H.; Thess, A.; Smalley, R. E. *Nature* **1997**, *386*, 474.
(17) Collins, P. G.; Zettl, A.; Bando, H.; Thess, A.; Smalley, R. E. *Science* **1997**, *278*, 100.
(18) Treacy, M. J.; Ebbesen, T. W.; Gibson, J. M. *Nature* **1996**, *381*, 678.
(19) Meyer, R. R.; Sloan, J.; Dunin-Borkowski, R. E.; Kirkland, A. I.; Novotny, M. C.; Bailey, S. R.; Hutchinson, J. L.; Green, M. L. *Science* **2000**, *289*, 1324.
(20) Halls, M. D.; Schlegel H. B. *J. Phys. Chem. B* **2002**, *106*, 1921.
(21) Hafner, J. H.; Bronikowski, M. J.; Azamian, B. R.; Nikolaev, P.; Rinzler, A. G.; Colbert, D. T.; Smith, K. A.; Smalley, R. E. *Chem. Phys. Lett.* **1998**, *296*, 195.
(22) Nikolaev, P.; Bronikowski, M. J.; Bradley, R. K.; Rohmund, F.; Colbert, D. T.; Smith, K. A.; Smalley, R. E. *Chem. Phys. Lett.* **1999**, *313*, 91.
(23) Chiang, I. W.; Brinson, B. E.; Huang, A. Y.; Willis, P. A.; Bronikowski, M. J.; Margrave, J. L.; Smalley, R. E.; Hauge, R. H. *J. Phys. Chem. B* **2001**, *105*, 8297.
(24) Bladh, K.; Falk, L. K. L.; Rohmund, F. *Appl. Phys. A* **2000**, *70*, 317.
(25) Kitiyanan, B.; Alvarez, W. E.; Harwell, J. H.; Resasco, D. E. *Chem. Phys. Lett.* **2000**, *317*, 497.
(26) Roland, C.; Bernholc, J.; Brabec, C.; Nardelli, M. B.; Maiti, A. *Mol. Simul.* **2000**, *25*, 1.
(27) Vander Wal, R. L.; Ticich, T. M.; Curtis, V. E. *J. Phys. Chem. A* **2000**, *104*, 7209.
(28) Li, G.; Bosio, S. B. M.; Hase, W. L. *J. Mol. Struct.* **2000**, *556*, 43.
(29) Billeter, S. R.; Hanser, C. F. W.; Mordasini, T. Z.; Scholten, M.; Thiel, W.; van Gunsteren, W. F. *Phys. Chem. Chem. Phys.* **2001**, *3*, 688.
(30) Bauschlicher, C. W. *Nano Lett.* **2001**, *1* (5), 223.
(31) Dubat, P.; Cenedese, P. *Phys. Rev. B* **2001**, *63*, 241402.
(32) Dewar, M. J. S.; Zoebisch, E.; Healy, E. F.; Stewart, J. J. P. *J. Am. Chem. Soc.* **1985**, *107*, 3902.
(33) Stewart, J. J. P. *J. Comput. Chem.* **1989**, *10*, 209.
(34) Mann, D. J.; Hase, W. L. *Phys. Chem. Chem. Phys.* **2001**, *19*, 4376.
(35) Lee, Y. H.; Kim, S. G.; Tomanek, D. *Phys. Rev. Lett.* **1997**, *78*, 2393.
(36) Andriotis, A. N.; Menon, M.; Froudakis, G. *Phys. Rev. Lett.* **2000**, *85*, 3193.
(37) Charlier, J. C.; Allesandro, D. V.; Blase, X.; Car, R. *Science* **1997**, *275*, 646.
(38) Hernandez, J.; Ordejon, P.; Boustani, I.; Rubio, A.; Alonso, J. A. *J. Chem. Phys.* **2000**, *111*, 3814.
(39) Schmidt, M. W.; Baldridge, K. K.; Boatz, J. A.; Elbert, S. T.; Gordon, M. S.; Jensen, J. J.; Koseki, S.; Matsunaga, N.; Nguyen, K. A.; Su, S.; Windus, T. L.; Dupuis, M.; Montgomery, J. A. *J. Comput. Chem.* **1993**, *14*, 1347.
(40) Hase, W. L.; Duchovic, R. J.; Hu, X.; Komornicki, A.; Lim, K. F.; Lu, D.-H.; Peslherbe, G. H.; Swamy, K. N.; Vande Linde, S. R.; Varandas, A.; Wang, H.; Wolf, R. J. *QCPE* **1996**, *16*, 671.
(41) Martyna, G. J.; Klein, M. L.; Tuckerman, M. *J. Chem. Phys.* **1992**, *97*, 2635.
(42) Jang, S.; Voth, G. A. *J. Chem. Phys.* **1997**, *107*, 9514.
(43) Schlegel, H. B. *J. Comput. Chem.* **1982**, *3*, 214.
(44) Chapman, S.; Bunker, D. L. *J. Chem. Phys.* **1975**, *62*, 2890.
(45) Sloane, C. S.; Hase, W. L. *J. Chem. Phys.* **1977**, *66*, 1523.
(46) Hase, W. L.; Ludlow, D. M.; Wolf, R. J. *J. Phys. Chem.* **1981**, *85*, 958.
(47) Peslherbe, G. H.; Wang, H.; Hase, W. L. Monte Carlo Sampling for Classical Trajectory Simulations. In *Monte Carlo Methods in Chemical Physics*; Ferguson, D. M., Siepmann, J. I., Truhlar, D. G., Eds.; Advances in Chemical Physics, Vol. 105; Wiley: New York, 1999; p 171.
(48) Hase, W. L. Classical Trajectory Simulations: Initial Conditions. In *Encyclopedia of Computational Chemistry*; von Ragué Schleyer, P., Ed.; Wiley: New York, 1998; Vol 1, p 402.
(49) Carey, F. A. *Organic Chemistry*, 2nd ed.; McGraw-Hill: New York, 1992.
(50) Zhu, X. Y.; Lee, S. M.; Frauenheim, T. *Phys. Rev. Lett.* **2000**, *85*, 2757.
(51) Maiti, A.; Brabec, C. J.; Roland, C.; Bernholc, J. *Phys. Rev. B* **1995**, *52*, 14850.
(52) Gavillet, J.; Loiseau, A.; Journet, C.; Willaime, F.; Ducastelle, F.; Charlier, J.-C. *Phys. Rev. Lett.* **2001**, *87*, 275504.
(53) Kiang, C.-H. *J. Chem. Phys.* **2000**, *113*, 4763.
(54) Iijima, S.; Ajayan, P. M.; Ichihashi, T. *Phys. Rev. Lett.* **1992**, *69*, 3100.
(55) Thess, A.; Lee, R.; Nikolaev, P.; Dai, H.; Petit, P.; Robert, J.; Xu, C.; Lee, Y. H.; Kim, S. G.; Rinzler, A. G.; Colbert, D. T.; Scuseria, G. E.; Tomanek, D.; Fischer, J. E.; Smalley, R. E. *Science* **1996**, *273*, 483.
(56) Kresse, G.; Hafner, J. *J. Phys.: Condens. Matter* **1994**, *6*, 8245.
(57) Kresse, G.; Hafner, J. *Phys. Rev. B* **1993**, *47*, 558.